CHEMPHYSCHEM

DOI: 10.1002/cphc.200600306

The Cell-Penetrating Peptide TAT(48-60) Induces a Non-Lamellar Phase in DMPC Membranes

Sergii Afonin,[a] Alexander Frey,[b] Sybille Bayerl,[c] Dahlia Fischer,[b] Parvesh Wadhwani,[a] Sevil Weinkauf,[c] and Anne S. Ulrich*[a, b]

Cell-penetrating peptides (CPPs) are short polycationic sequences that can translocate into cells without disintegrating the plasma membrane. CPPs are useful tools for delivering cargo, but their molecular mechanism of crossing the lipid bilayer remains unclear. Here we study the interaction of the HIV-derived CPP TAT (48-60) with model membranes by solid-state NMR spectroscopy and electron microscopy. The peptide induces a pronounced isotropic ^{31}P NMR signal in zwitterionic DMPC, but not in anionic DMPG bilayers. Octaarginine and to a lesser extent octalysine have the same effect, in contrast to other cationic amphiphilic membrane-active peptides. The observed non-lamellar lipid morphology is attributed to specific interactions of polycationic peptides with phosphocholine head groups, rather than to electrostatic interactions. Freeze-fracture electron microscopy indicates that TAT(48-60) induces the formation of rodlike, presumably inverted micelles in DMPC, which may represent intermediates during the translocation across eukaryotic membranes.

Introduction

Biomembranes are generally impermeable to large or highly charged molecules. Pharmaceutical approaches for intracellular deposition of cargo have traditionally used viral vectors for gene therapy,[1–8] besides some physical methods to enhance internalization.[9–11] More recently, also non-viral carrier systems have become available for the delivery of drugs and DNA, such as polylysines, polyethylenimines, dendrimers, organically modified silicas, cyclodextrins and cationic liposomes.[7,9,12–15] Studies with polycationic peptides and peptoids have led to the identification of so-called cell-penetrating peptides (CPPs) as delivery vehicles, also known as transduction or Trojan peptides.[16–20] Some of these are derived from internal sequences of viral proteins (protein transduction domains), while others are rationally designed. These short polycationic peptides (typically 6–30 amino acids) are able to translocate across cellular membranes in a receptor-independent and often energy-independent manner, without disrupting their barrier function or affecting the integrity of the living cells. They are essentially non-toxic, exhibit low immunogenicity and thus are promising delivery systems.

Cell-penetrating peptides can carry various kinds of covalently and non-covalently attached cargo into cells, such as fluorescent labels, drugs, proteins, nucleic acids, peptide nucleic acids, nanoparticles, liposomes and virions.[17–20] Internalization occurs either directly across the plasma membrane or endocytotically.[21–35] Either route must proceed by some kind of transbilayer translocation, which is presumably an energy-independent step without the need for a specific receptor.[36] Therefore, to lay the foundation for rational design of more efficient CPPs, it is necessary to explore the mechanism of membrane translocation across pure lipid bilayers. Many efforts have been made to understand the role of peptide sequence, lipid composition, cargo and general physicochemical conditions that enable translocation.[20,23,26–28,30] Liposomes from natural lipid extracts or synthetic lipids are often used as protein-free artificial membrane systems, ideal for studying pure peptide–lipid interactions. For several CPPs, binding, membrane insertion, bilayer disruption, translocation and/or fusogenicity have been characterized in such model systems.[30,32,33,37–39] For example, some peptides derived from the HIV protein Tat (transacting activator of transcription) were shown to induce phospholipid mixing and vesicle fusion without detectable dye leakage, as seen by fluorescence.[32] Recently, it was also demonstrated that they can translocate through liposomes consisting of pure 1-palmitoyl-2-oleoyl-*sn*-glycero-3-phosphocholine (POPC)[33] and through giant vesicles consisting of soybean phosphatidylcholine, but not through large unilamellar ones.[30] Such studies contribute to a better understanding of the molecular aspects in the mechanism of translocation. Several hypotheses have been proposed but not yet proven: translocation may occur 1) via a transient peptidic pore (similar to cationic amphiphilic antimicrobial peptides),[40] 2) via a local molecular electroporation-like process,[41] 3) via the formation of inverted micellar

[a] *Dr. S. Afonin, Dr. P. Wadhwani, Prof. Dr. A. S. Ulrich*
Institute of Biological Interfaces, Forschungszentrum Karlsruhe
Hermann-von-Helmholtz-Platz 1
76344 Eggenstein-Leopoldshafen (Germany)
Fax: (+49) 721-608-4823,
E-mail: anne.ulrich@ibg.fzk.de

[b] *A. Frey, Dr. D. Fischer, Prof. Dr. A. S. Ulrich*
Institute of Organic Chemistry, Universität Karlsruhe (TH)
Fritz-Haber-Weg 6, 76131 Karlsruhe (Germany)

[c] *Dr. S. Bayerl, Prof. Dr. S. Weinkauf*
Department of Chemistry, Technische Universität München
Lichtenbergstr. 4, 85747 Garching (Germany)

lipid structures,[22] or 4) via an anion-mediated route.[42] In living systems, different internalization pathways and membrane translocation mechanisms may apply to different CPPs, depending also on the type of cargo and cell line.[23,43]

Here we examine the interactions of the CPP TAT(48-60),[21,24,26,28,33,35,36,44] with phospholipid model membranes. It is an arginine-rich sequence consisting of 13 amino acids (GRKKRRQRRRPPQ), derived from the basic domain of the HIV-1 protein Tat (to distinguish the parent protein "Tat" from the derived peptide "TAT" we use these different forms of capitalization throughout the text). The well-known translocation function of the parent protein is attributed to the region involving amino acids 44–61. In the literature, a range of sequences are denoted as Tat-CPP, with a consensus over 48–57, as included in our peptide. TAT(48-60) belongs to the group of polar non-amphiphilic CPPs, which amongst others, includes polycations such as Arg_n, Lys_n, Orn_n, His_n; guanidinium-rich peptoids; β-peptides; peptide nucleic acids; and carbamate oligomers.[14,25,27,28,30,32,36,42,45–47] Since these linear or branched molecules carry multiple positive charges over a wide physiological pH range, their spontaneous membrane translocation is rather surprising from a physical point of view. Internalization of Tat-CPPs and their analogues was initially suggested to involve a non-endocytotic pathway,[23,24,27] though later it was proposed to proceed via a special endocytosis-related route that is lipid-raft- or glucosaminoglycan-mediated.[21,26–28,36,43] However, as the findings depend strongly on the cell model used, the molecular mechanism of translocation—especially the final step across the lipid bilayer—still remains unclear.[36] In contrast to these highly charged polar molecules, a rather different class of CPPs has primary or secondary amphiphilic nature, such as transportan, *Drosophila antennapedia* transcription factor, Herpes simplex virus type-1 VP22 transcription factor and the "model amphiphilic peptide" MAP. The physicochemical nature of those peptides makes them intuitively capable of inserting into the hydrophobic core of the lipid bilayer. Hence, the membrane translocation mechanism of amphiphilic CPPs may differ intrinsically from that of the polar non-amphiphilic CPPs like TAT(48-60).

To examine the effect of TAT(48-60) on model membranes, we used solid-state ^{31}P NMR spectroscopy and freeze-fracture transmission electron microscopy (TEM) to characterize the morphology of several different lipid/peptide samples.[48–51] Lipid polymorphism is conveniently reflected in the ^{31}P NMR spectra of the phospholipid head groups. Motional averaging of the ^{31}P chemical shift anisotropy leads to three principally different types of line shape that depend on the local geometry over which lipid diffusion occurs. The characteristic line shapes are used to identify and quantify lamellar, hexagonal and "isotropic" lipid mesophases, as are typically observed in model and natural membranes under biologically relevant conditions.[48,49,51] In the case of an isotropic ^{31}P NMR signal, however, it is not possible to discriminate between micelles, small vesicles and cubic phases. On the other hand, TEM, can provide a direct picture of the lipid morphology complementary to ^{31}P NMR spectroscopy, and thus allows multilamellar stacks and vesicles of different sizes, as well as hexagonal and cubic phases, to be distinguished in a semi-quantitative manner.[50]

Here, we provide evidence by ^{31}P NMR spectroscopy that the cell-penetrating peptide sequences TAT(48-60), Arg_8 and Lys_8 can induce formation of an isotropic phase in model membranes containing the lipid 1,2-dimyristoyl-*sn*-glycero-3-phosphocholine (DMPC). A comparison of different lipid head groups and chains reveals some specific interactions of these polar polycationic CPPs that are not exhibited by amphiphilic cationic peptides. TEM suggests a non-lamellar lipid morphology of short rod-shaped micelles. We thus support the concept that the translocation mechanism of polar CPPs can proceed via formation of inverted micelles.

Results

Solid-State ^{31}P NMR of TAT(48-60) interacting with DMPC

Concentration Dependence

In an early ^{31}P NMR study on TAT(47-57), Ziegler et al.[52] examined POPC/POPG (3/1 mol/mol) multilamellar vesicles to study its membrane interactions. The mixed phospholipids exhibited a powder pattern with uniform chemical shift anisotropy indicative of a lamellar bilayer phase. Upon addition of the CPP an increase in the spectral span ($\sigma_{||}-\sigma_{\perp}$) was observed. This change was found to be proportional to the molar peptide/lipid ratio (P/L) of the CPP to the negatively charged lipid 1-palmitoyl-2-oleoyl-*sn*-glycero-3-[phospho-*rac*-(1-glycerol)] (POPG). The maximal effect occurred at about 1/4, corresponding to a total peptide/lipid ratio of P/L = 1:16. In our first experiments we wanted to reproduce these findings with saturated phospholipids; hence, we started with a control sample of pure, uncharged DMPC. Surprisingly, in the presence of TAT-(48-60) the ^{31}P NMR spectra of DMPC exhibited a pronounced isotropic signal at about 0 ppm which had not been reported before. It is indicative of an "isotropic" lipid morphology, such as micelles, very small vesicles or cubic phases, in which the lipids diffuse rapidly around all directions in space. Figure 1 il-

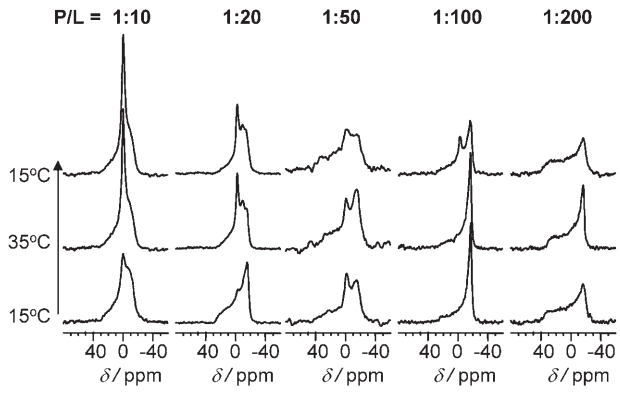

Figure 1. ^{31}P NMR spectra of DMPC in the presence of different amounts of TAT(48-60), as indicated by the molar peptide/lipid ratio P/L. Samples were measured in a temperature series as described in the Experimental Section. Only the spectra at the lowest (15 °C, bottom, top rows) and highest (35 °C, middle row) temperatures are shown. The direction of temperature change is indicated by the arrow.

lustrates the concentration dependence of this effect in a series of samples with the P/L ratio varying from 1/10 (10 mol% peptide) down to 1/200 (0.5 mol%). The isotropic component was found to be somewhat irreproducible in fresh samples (bottom row), but it become more pronounced upon cycling the sample through the main lipid phase transition temperature $T_m = 23.6\,^{\circ}C$ for DMPC (top row). Representative ^{31}P NMR spectra in Figure 1 are thus illustrated for the gel phase at 15 °C (start of the experiment), the liquid-crystalline phase at 35 °C (1st heating) and again at 15 °C (1st cooling). It can be seen from the top row of Figure 1 that the TAT(48–60)-induced isotropic lipid phase occurs for P/L ratios as low as 1/100, and it increases with increasing peptide concentration.

Detailed Thermal History of the Sample

Our first attempts to quantify the isotropic ^{31}P NMR signal were hampered by poor reproducibility of the peptide-induced effect, until we realized the importance of controlling the thermal history of the sample: Repeated cycling through the lipid phase transition temperature T_m brought about the desired reproducibility, rather than any incubation at extreme temperatures or freeze–thaw treatment. Figure 2 illustrates the detailed temperature dependence of a representative DMPC sample with TAT(48-60) at a P/L ratio of 1/20. This sample was hydrated to 75% (v/w) at 40 °C with an aqueous solution of the peptide and cooled to the gel phase for transport and handling, and the NMR experiments were started at 15 °C (see Experimental Section). The spectra were measured in a quasicontinuous temperature series over 1° steps (ca. 5 min per spectrum) to give reproducible results in repeated experiments with different samples and different batches of peptide. Figure 2

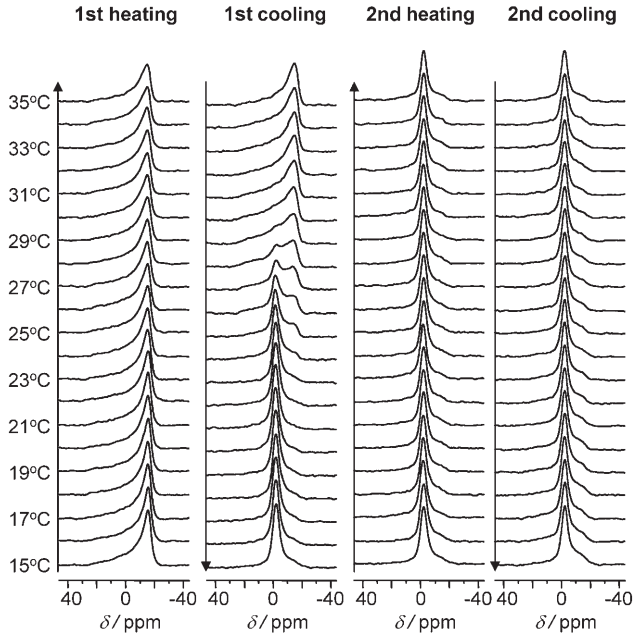

Figure 2. Temperature series of ^{31}P NMR spectra of DMPC in the presence of TAT(48-60) at P/L = 1/20, as described in the Experimental Section. Directions of temperature change are indicated by arrows.

shows that in the 1st heating series only the lamellar lipid phase prevails and no isotropic signal occurs. Notably, the spectral span ($\sigma_{||} - \sigma_{\perp} = 34$ ppm) of the lamellar signal is smaller than that of pure DMPC (ca. 45 ppm,[48,49,51] see Figure 3A).

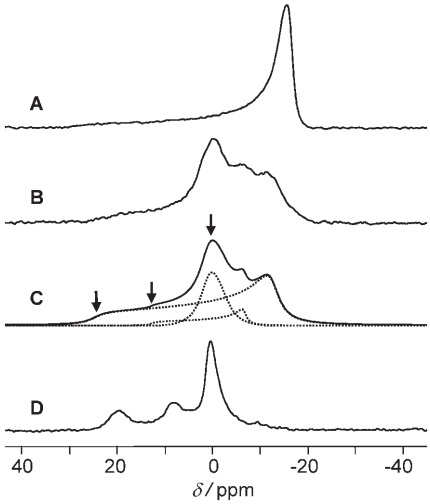

Figure 3. Experimental (A, B, D) and simulated (C) ^{31}P NMR spectra of DMPC in the presence of TAT(48-60) at 35 °C. A) Control spectrum of pure DMPC. B) DMPC/TAT(48-60) at P/L = 1/20. C) Full line-shape deconvolution of spectrum B) assuming three components (two lamellar phases and one narrow hexagonal phase). Fits of the individual phases (dotted lines) and their sum (solid line) are shown. Arrows indicate the positions where a signal would be expected in the corresponding oriented sample. D) Macroscopically oriented DMPC/TAT(48-60) sample with the membrane normal parallel to the magnetic field.

In the 1st cooling series, however, the isotropic ^{31}P NMR signal appears and grows from 29 to 23 °C (i.e., around the lipid $L_\alpha/P_{\beta'}$ phase transition temperature). Once the non-lamellar phase has formed in the gel phase, it is irreversible and retains its intensity in subsequent heating and cooling cycles. In principle, the bottom spectrum in the second column of Figure 2 should be identical to the top spectrum in the second column (P/L = 1/20) of Figure 1. However, close inspection reveals that these similarities are only of a qualitative nature, due to slight differences in the treatment and thermal history of the individual samples prepared at different times. Therefore, in all series of samples that were to be compared directly with one another, we took special care to process all of them identically at the same time, and thus make them amenable to quantitative comparison within a single figure.

^{31}P NMR Line-Shape Deconvolution

Close inspection of the ^{31}P NMR data of Figure 1 reveals that the line shapes contain not only a broad lamellar plus an isotropic component, but another, narrower lamellar signal is present as well. This component is clearly seen in the powder spectrum of DMPC containing TAT(48-60) at P/L = 1/20 in Figure 3B. To confirm the nature of these three distinct components, we also prepared a macroscopically oriented NMR sample with the same composition. Inspection of the corresponding spectrum in Figure 3D indeed shows three narrow

resonances at 19, 7 and 0 ppm, fully supporting the expected two lamellar phases plus one isotropic component.[1] All ^{31}P NMR powder spectra were thus deconvoluted by line-shape simulation accordingly, giving CSA values of $\sigma_{||} =$ 23.6 ppm and $\sigma_{\perp} = -10$ ppm for the broad lamellar component, and $\sigma_{||} = 11.8$ ppm and $\sigma_{\perp} = -3.5$ ppm for the narrower one. The isotropic signal was readily fitted by a Lorentzian line of 2.4 ppm width at half height. Notably, when no constraints were imposed on its center frequency, best fits were obtained with the signal shifted by about 1–3 ppm downfield from the corresponding isotropic value of the two lamellar signals. Indistinguishably good fits were also obtained with a very narrow (but unshifted) hexagonal line shape instead of a shifted Lorentzian.

Comparison of the Interactions of TAT(48-60) with Different Types of Lipids

Influence of Negatively Charged DMPG

In view of the polycationic nature of TAT(48-60), most previous studies focussed on membranes with a high content of negatively charged lipids.[30,32,33,52] Hence we also prepared mixed DMPC/DMPG (1,2-dimyristoyl-*sn*-glycero-3-[phospho-*rac*-(1-glycerol)]) samples with a constant P/L ratio of 1/20, varying the molar percentage of DMPG over a range of 0, 10, 30, 50 and 100%. Both lipids have been well characterized with regard to their physicochemical behaviour; they are highly miscible and exhibit similar phase transition temperatures (L_{β}/$P_{\beta'}$ at 13.4 °C for DMPC and 12.5 °C for DMPG, $P_{\beta'}$/L_{α} at 23.6 °C for DMPC and 23.3 °C for DMPG[53,54]). Figure 4 shows that all

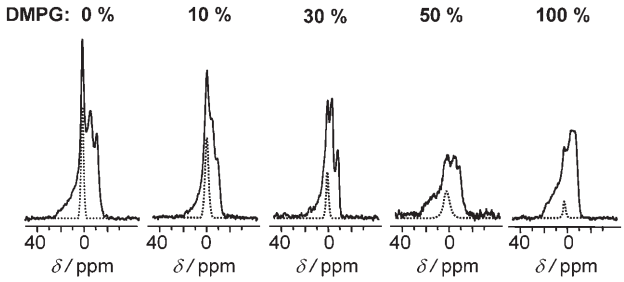

Figure 4. ^{31}P NMR spectra of DMPC/DMPG mixtures containing TAT(48-60) at P/L = 1/20 at 35 °C.

spectra of the mixed lipid systems with TAT(48-60) exhibit the three ^{31}P NMR signals described above. However, the isotropic component decreases significantly with increasing DMPG content, as seen from the superimposed line-shape simulations, whose integral intensity decreases from about 40 to 2% of the total spectral area. These values were found to be reproducible to within about 20% of each relative amount when four separately prepared series of DMPC/DMPG samples were compared by using different batches of TAT(48-60) with water contents of 75 and 50% and applying isotropic or narrow hexagonal fits. In contrast to the isotropic ^{31}P NMR signal, we note that the narrower lamellar component is always observed in the presence of the peptide at a P/L ratio of 1/20. In some series of measurements (data not shown) we observed that the intensity of this component increased at the expense of the isotropic one.

[1] *We note that the line positions in Figure 3D do not exactly coincide with the expected frequencies from the non-oriented samples (see arrows in Figure 3B), but these slight shifts are attributed to differences in water content. The lipid dispersions (75% v/w water) contain an excess of water, while the oriented samples were incubated at 96% relative humidity.*

Phosphatidylcholines with Different Acyl Chains

Next we compared the interaction of TAT(48-60) with phosphatidylcholines containing different acyl chains. Since the isotropic ^{31}P NMR signal is induced by passage through the lipid phase transition, the corresponding thermocycles of these samples were designed to start about 10 °C below and end about 10 °C above the respective T_m.[54] Figure 5 shows that

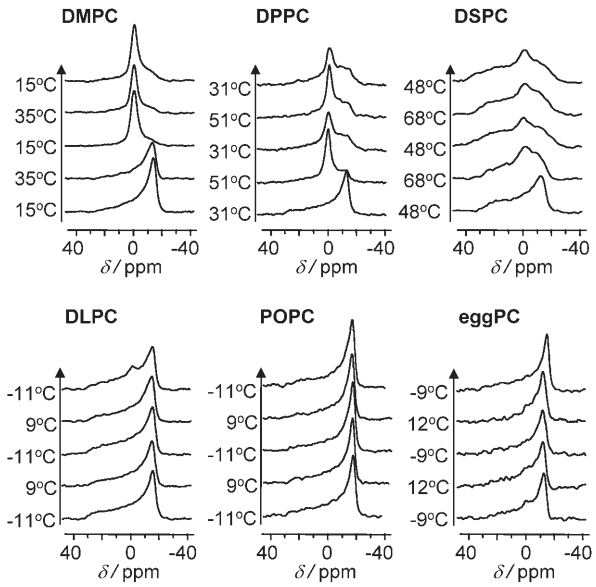

Figure 5. ^{31}P NMR spectra of different phospholipids in the presence of TAT-(48-60) at P/L = 1/20. Each sample was measured in a temperature series (see Experimental Section) around T_m of the corresponding lipid. Only the spectra at the highest and lowest temperatures are shown. The temperatures and directions of change are indicated.

TAT(48-60) at a P/L ratio of 1/20 induces a non-lamellar phase in all saturated phosphatidylcholines, although to different extents depending on acyl chain length. In DMPC ($T_m = 23.6$ °C), DPPC (1,2-dipalmitoyl-*sn*-glycero-3-phosphocholine, $T_m =$ 41.3 °C) and DSPC (1,2-distearoyl-*sn*-glycero-3-phosphocholine, $T_m = 54.5$ °C) the effect is most pronounced, whereas in DLPC (1,2-lauroyl-*sn*-glycero-3-phosphocholine, $T_m = -1.9$ °C) it is much less so. The low-melting, unsaturated lipids POPC (1-palmitoyl-2-oleoyl-*sn*-glycero-3-phosphocholine, $T_m = -2.5$ °C) and eggPC (egg yolk phosphatidylcholines, T_m very broad around 0 °C) do not exhibit any significant isotropic signal.

Comparison of Other Cationic Membrane-Active Peptides in DMPC

To clarify whether the induction of the non-lamellar lipid phase is a unique feature of TAT(48-60), we examined a wide range of other membrane-active peptides in DMPC at P/L = 1/10, prepared in the same way as described in the Experimental Section. Figure 6 illustrates the results for samples containing the octapeptides Arg_8 and Lys_8, which carry the same net charge

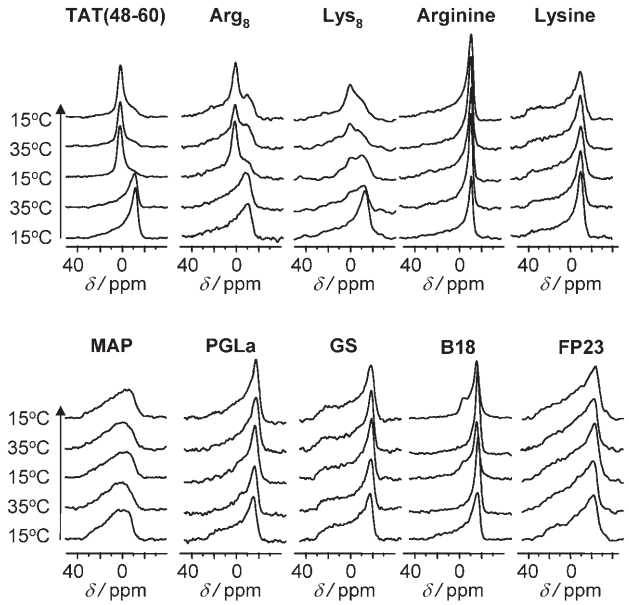

Figure 6. ^{31}P NMR spectra of DMPC in the presence of different membrane-active cationic peptides (and amino acids as controls). For all samples a P/L ratio of 1/10 was used, except for TAT(48-60), prepared at P/L = 1/20. Only the spectra at the highest and lowest temperatures of the series are shown.

as TAT(48-60) with 6 Arg and 2 Lys. Notably Arg_8, which is most similar to the TAT(48-60) sequence, induces an isotropic ^{31}P NMR signal with almost the same intensity, and Lys_8 does so to a lesser extent. Control experiments with the respective pure amino acids did not show any such effect. A different kind of cell-penetrating peptide, the so-called MAP (model amphiphilic peptide, KLALKLALKALKAALKLA-NH_2)[29] was also included in the comparison. In contrast to the polar TAT(48-60) peptide, MAP belongs to the class of amphiphilic CPPs and carries six positive charges in its α-helical structure. Figure 6 clearly shows that MAP has no effect on the ^{31}P NMR line shape of DMPC. Next, some representative cationic amphiphilic peptides were tested, which are well known for their antimicrobial membrane-disruptive function. PGLa (GMASKAGAIAG-KIAKVALKAL-NH_2),[55–59] which has a similar amphiphilic α-helical structure to MAP, shows no effect on DMPC, and neither does gramicidin S [*cyclo*-(PVOL^{D}F)$_2$],[55,56,60–62] which has an amhiphiphilic β-sheet structure. Finally, two fusogenic peptides were examined, namely, B18 (LGLLLRHLRHHSNLLANI) from a sea urchin fertilization protein[55,56,63–65] and FP23 (AVGIGALFLGFL-GAAGSTMGARS-NH_2) from the C-terminus of the HIV-1 fusion protein gp41.[66] Of these two peptides, only B18 shows a small effect on the ^{31}P NMR lineshape, which is interesting to note, as this peptide contains two Arg residues. It also seems that the features of the powder line shapes of the various samples in Figure 6 represent vesicle shapes that deviate from spherical symmetry. This finding is attributed to interactions with peptide structures having different susceptibilities in the strong magnetic field.[67] Overall, the absence of the distinct isotropic ^{31}P NMR signal for all but the polar non-amphiphilic CPPs TAT-(48-60), Arg_8 and Lys_8, suggests that a certain charge density and/or three-dimensional charge distribution is required for the observed effect on DMPC.

Transmission Electron Microscopy of DMPC Containing TAT(48-60)

To visualize the morphology of TAT(48-60)-containing membranes directly, freeze-fracture TEM images were obtained on the same DMPC sample that was used for ^{31}P NMR (P/L = 1/20, see Figure 1). Representative TEM images show a distribution of uni- and multilamellar liposomes (data not shown here) besides extended lamellar stacks, which are all consistent with a lamellar ^{31}P NMR line shape. Neither cubic nor classical hexagonal phases were detected. The TEM images, however, also contain many fragmented bilayer patches which are interspersed with an unusual lipid morphology, illustrated in Figure 7 A.

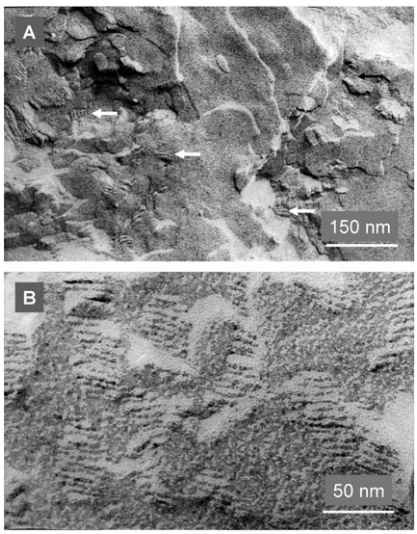

Figure 7. Freeze-fracture electron micrograph of DMPC containing TAT(48-60) at P/L = 1/20 (A) and enlarged image of the rod-like lipid assemblies (B).

Magnification (Figure 7 B) reveals small bundles with a spacing of about 5 nm, whose appearance suggests that they consist of short rod-like lipid assemblies. We interpret the observed structures as lipid micelles, which are presumably inverted as they are assembled in bundles. This kind of morphology clearly differs from the long cylinders of the classical hexagonal phases, and to our knowledge has not been described before.

Discussion

The observation that the cell-penetrating peptide TAT(48-60) and its analogue Arg_8 induce a pronounced isotropic ^{31}P NMR signal in DMPC was unexpected and exciting for two reasons. First, previous publications had ignored the ubiquitous phosphocholine head group as a candidate for interactions due to its electroneutral nature. Second, the isotropic line shape suggests the formation of micelles or other unusual lipid morphologies, which could be the relevant intermediate structures involved in the translocation of TAT(48-60) across cellular membranes. The most intriguing question concerns the origin and morphological interpretation of the isotropic ^{31}P NMR component (Figure 1), which was addressed by freeze-fracture electron microscopy (Figure 7). The TEM images show a wide size distribution of uni- and multilamellar liposomes besides extended lamellar stacks, and hence the formation of a discrete population of very small lipid vesicles can be excluded. Neither are cubic phases detected. Extensive fragmentation of the membranes into free micelles (with positive curvature) is also unlikely, since the oriented NMR sample with a low water content would not have provided the necessary bulk hydration to accommodate these. Instead, the TEM images reveal bundles of elongated structures with a packing distance of 5 nm. They are embedded in the multilamellar stacks and appear to represent rod-like micelles that are presumably inverted. This interpretation matches the observations by ^{31}P NMR spectroscopy, since the "isotropic" signal can be fitted by a very narrow hexagonal line shape just as well as by a Lorentzian line that is shifted downfield by a few parts per million. In view of the TEM results, we prefer the first interpretation of the ^{31}P NMR signal in terms of a very narrow hexagonal line shape, as this is fully explicable by the shape of an elongated micelle, and it does not require any reasoning as to why an isotropic Lorentzian line should be shifted by interaction with the peptide. Such slightly elongated lipidic structures, which are consistent with both TEM and ^{31}P NMR results, may thus provide an explanation for the translocation mechanism of TAT(48-60) across lipid membranes as being mediated by inverted micelles.

As in most other previous studies on polycationic CPPs, we had initially assumed that a negative charge is required in the target membrane for peptide–lipid interactions to occur. The TAT(48-60) peptide carries a net charge of $+8$ and is therefore expected to interact electrostatically with negatively charged lipid head groups such as phosphoglycerol. When comparing the ^{31}P NMR spectra of DMPC/DMPG lipid mixtures (Figure 4), however, we found—contrary to these expectations—that the intensity of the isotropic ^{31}P NMR signal decreases with increasing content of DMPG. TAT(48-60) induces hardly any isotropic signal in 100% DMPG, which remains mostly lamellar over a wide range of peptide concentrations and temperatures. This observation suggests that electrostatic interactions of DMPG with TAT(48-60) may compensate or shield the active sites of the peptide from their otherwise perturbing contacts with the zwitterionic phosphocholine head groups. The most likely candidates for these specific peptide–lipid interactions are the arginine and lysine side chains. Our ^{31}P NMR experiments with the corresponding octapeptides demonstrated that Arg_8 induces virtually the same degree of perturbation in DMPC as TAT-(48-60), while Lys_8 has a lesser effect (Figure 6). These observations are in good agreement with earlier findings that the biological transduction efficiency decreases in the order $Arg_8 >$ Tat-CPPs $> Lys_8$.[68] Likewise, it has been reported that a Tat CPP in which all charged side chains were substituted as Arg is much more active than the corresponding analogue containing only Lys side chains.[28,30] Concerning the specific molecular interactions between TAT(48-60) and DMPC, it is likely that the arginine side chains form bidentate complexes with the lipid phosphate groups via their guanidinium moieties. Phosphate ions are known to be able to shield the charges of arginine-rich peptides and enable their transfer between bulk water and $CHCl_3$.[45] Likewise, molecular dynamics simulations have shown hydrogen bonds between guanidinium and phospholipid head groups.[69] These strong interactions thus seem to trigger the formation of the peptide-induced isotropic lipid phase in DMPC reported here.

Interestingly, the TAT(48-60)-induced effects on the lipid morphology are rather sensitive to the sample preparation protocol, in particular to the thermal history of the hydrated peptide–lipid dispersion. Reproducible results were obtained by adding a peptide solution to a dry lipid preparation at elevated temperature, and by thermocycling this metastable sample up and down through the lipid-chain melting transition (Figure 2). Once the peptide is wrapped up in the proposed inverted lipid micelles, the isotropic lipid phase remains stable. We can thus suggest that the intimate contact of TAT-(48-60) with its lipid partners is promoted by membrane defects which make the hydrophobic bilayer interior accessible and are most abundant at the main-phase transition temperature T_m. Yet, it appears that subtle differences in the lipid-chain melting process may influence the extent to which TAT(48-60) is able to perturb lipids with different types of acyl chains (Figure 5). Saturated phosphatidylcholines with an ambient T_m (DMPC, DPPC, DSPC) were found to exhibit a significant isotropic lipid signal, and this suggests that TAT(48-60) can induce and enter the inverted micellar structures readily when presented with bilayer defects. In contrast, this effect was not observed in lipids with a T_m close to or below 0 °C (DLPC, DOPC, eggPC), irrespective of their degree of chain saturation. In these samples, the formation of ice or a freezing-induced segregation of the peptide seems to have prevented its redistributing and entering any available bilayer defects. Turning our attention to real biological membranes, it may be argued that they are usually liquid-crystalline under ambient conditions and do not experience any phase transitions; hence, the observed lipidic structures may not be relevant in vivo. However, even living cells are likely to carry many defects in their membranes, for example, at the domain boundaries of lipid rafts, near the lipid annulus of certain transmembrane proteins, and possibly also induced by the peripheral binding of peptides themselves. Furthermore, amongst many examples, the cytotoxic equinatoxin and the fusogenic protein of the Semliki Forest virus are known to require sphingomyelin in the target cell, which prefers a gel phase, especially when localized to

lipid rafts.[70,71] Hence, it is not unusual for a membrane-perturbing process to be activated by specific interactions with the inconspicuous phosphocholine head group of a saturated lipid.

Our observations on the role of sample preparation and transient bilayer defects when cycling the temperature though T_m may have some implications for the interpretation of previous controversial results in living cells. If a local (dis)integrity of the lipid bilayer is critical, experimental differences may be due not only to the now well-recognized artefacts of cell fixation,[31] but also to many other parameters such as temperature, medium, and so on. Furthermore, it has been demonstrated that TAT CPPs and the Tat protein itself utilize a raft mechanism rather than the classic clathrin-mediated endocytotic route.[34,35] This finding suggests a crucial function for certain lipid types and a potential role of lipid phase boundaries, which may vary between cell types and depend on the conditions of cell cultivation. Of course we are not able to speculate whether the peptide is internalized directly across the plasma membrane or following endocytosis,[23,36] but our findings suggest that the TAT(48-60)-induced isotropic lipid phase is restricted to certain lipid species which would presumably have to accumulate locally at the site of entry.

Going back to our initial ^{31}P NMR observations, it appeared surprising that the cationic TAT(48-60) peptide was able to exert such a dramatic influence on the packing of the lipid acyl chains via interaction with the zwitterionic DMPC head groups. We therefore also tested a range of other cationic membrane-active peptides by preparing samples in the same way and using a high peptide/lipid ratio of 1/10. None of these representative peptides induced any comparable isotropic ^{31}P NMR signals in DMPC, including the cell-penetrating peptide MAP, the antimicrobial peptides PGLa and gramicidin S and the fusogenic peptide FP23 (Figure 6). Notably, all these peptides are amphiphilic and membrane-active. In contrast, TAT(48-60), Arg_8 and Lys_8 are polar rather than amphiphilic, irrespective of the fact that they only carry a slightly higher charge (+8) than the cell-penetrating peptide MAP (+6). Amphiphilic CPPs are thus unlikely to form inverted micelles, but they may instead translocate via the transient formation of peptidic pores, as suggested before.[16,18] In contrast, other polar polycationic peptides and proteins related to the Tat family may utilize the inverted-micellar mechanism implied here. For this to occur, it would appear necessary that 1) intimate complexes be formed between the lipid phosphate groups and preferentially some arginine side chains, which may be 2) favoured by lipid-bilayer defects that make the hydrophobic bilayer interior transiently accessible to one side. Furthermore, 3) the linear peptide sequence must engage locally in a sufficiently large number of interactions, so that 4) this perturbation and possibly the resulting dehydration impose a high curvature on the lipid head groups. As a consequence, the lipids could form inverted micelles, which 5) thereafter allow the CPP to translocate across the remaining lamellar part of the lipid bilayer without leakage.

Conclusions

The main message of this study is that the cell-penetrating peptides TAT(48-60) and Arg_8, and to a lesser extent also Lys_8, can induce an isotropic ^{31}P NMR signal in DMPC membranes. It is attributed to the formation of short rod-like lipid micelles, which are presumably inverted and assemble into bundles, as seen by electron microscopy. The isotropic ^{31}P NMR signal could be analyzed quantitatively after cycling the sample through the lipid-chain melting temperature, and was found to be proportional to the peptide/lipid ratio. An isotropic signal was also observed in other saturated phosphatidylcholines, but it was successively diminished by the addition of increasing amounts of negatively charged DMPG. The molecular interactions responsible for the formation of the isotropic lipid phase seem to involve complexes between the phosphate groups and the arginine side chains (and to a lesser extent lysine). We conclude that the unusual rod-like micellar structures observed here may be related to the cell-penetrating activity of the polar polycationic TAT(48-60) across lipid bilayers. Other cationic but amphiphilic membrane-active peptides, on the other hand, do not show such ^{31}P NMR characteristics and presumably follow a different translocation route into cells, for example, via peptidic pores.

Experimental Section

Peptides and Lipids: The TAT(48-60) peptide (GRKKRRQRRRPPQ), Arg_8 (RRRRRRRR) and Lys_8 (KKKKKKKK) were synthesized by using standard solid-phase Fmoc protocols on an Applied Biosystems (Forster City, CA) 433A instrument. The Wang resins, Fmoc-protected amino acids, *N*,*N*-diisopropylethylamine, 6-chloro-1-hydroxybenzotriazole and 2-(1*H*-6-chlorobenzotriazole-1-yl)-1,1,3,3,-tetramethyluronium hexafluorophosphate were obtained from Merck (Schwalbach, Germany), and dimethylformamide, piperidine and trifluoroacetic acid (TFA) from Sigma–Aldrich (Taufkirchen, Germany). TFA-cleaved crude peptides were purified with a linear H_2O/acetonitrile gradient on a C18 Grace Vydac (Hesperia, CA) HPLC column (10 × 250 mm) with HCl (5 M^{-3}) or TFA (0.125% v/v) as ion-pairing agents in both solvents. Peptide purity (>98%) was confirmed by using the same gradient on an analytical C18 Grace Vydac HPLC column (4.6 × 250 mm). The correct peptide mass was confirmed by MALDI-TOF MS on a Bruker Biflex-IV instrument (Bremen, Germany). Other synthetic peptides used in the study (MAP, PGLa, gramicidin S, B18 and FP23) were synthesized and purified as described earlier.[52–55] The lipids DMPC, DLPC, DPPC, DSPC, POPC, DMPG and eggPC were purchased from Avanti Polar Lipids (Alabaster, AL) and used without further purification.

Solid-State NMR Samples: NMR samples, unless otherwise stated, were prepared as lipid dispersions (75% v/w water content). Lipid solutions (in MeOH/$CHCl_3$, 1/2 v/v) were dried under a stream of N_2 and subsequently under vacuum. The dry lipid was hydrated (40 min) at 15 °C above the respective lipid phase transition temperature (T_m) by adding either water (for the control samples) or an aqueous solution of TAT(48-60) and vortexing the suspension thoroughly every 10 min. In the hydration solution the peptide was present in a concentration to achieve molar peptide/lipid ratios P/L of 1/10, 1/20, 1/50, 1/100 or 1/200. For the 1/20 samples, typically 1.5 mg peptide and about 12 mg of lipid were used. [The samples were prepared by weighing out the lyophilized peptides,

and control experiments demonstrated the same quantitative ^{31}P NMR effects for different batches of TAT(48-60) purified with either TFA or HCl, when taking into account the correspondingly different masses of the ion-paired complexes TAT(48-60)·9 CF_3COO^- vs TAT(48-60)·9 Cl^-]. The hydrated peptide/lipid dispersions were pipetted into a plastic bag, heat-sealed and immediately used for the NMR measurements. Special care was taken to keep the samples below T_m prior to the NMR measurements. Some of the lipid dispersion samples of TAT(48–60) in DMPC/DMPG (where noted) were prepared in a different way, giving a water content of 50%. Here the appropriate peptide/lipid mixture (in 70% MeOH) was prepared first, then dried and finally hydrated with water (30 min at 50 °C) with occasional vortexing. The macroscopically oriented NMR sample was prepared by co-dissolving the peptide and DMPC in MeOH/$CHCl_3$ (1/2 v/v) by the method described earlier.[56–59,61,62,65,72] Briefly, the solution was spread onto glass plates, air-dried and vacuum-dried (>8 h). The plates were stacked and hydrated in a humid chamber for at least 24 h at 96% relative humidity (over K_2SO_4 at 48 °C) and finally wrapped with Parafilm and polyethylene foil.

^{31}P NMR Spectroscopy: Solid-state ^{31}P NMR spectra were acquired on a Bruker (Karlsruhe, Germany) AVANCE spectrometer at 202.5 MHz. Spectra were recorded using a Hahn echo sequence with TPPM-20 ^{1}H decoupling, 90° pulse lengths of 7.2 μs, echo-delay times of 30 μs and a recycle time of 2 s. Each spectrum was acquired with 128 scans and processed with 100 Hz line broadening. Unless otherwise stated, the following temperature series was measured: a) heating, b) cooling, c) heating, d) cooling. The temperature ranges were chosen to start at about 10 °C below the respective T_m up to about 10 °C above T_m. The temperature was changed in 1 °C steps, and the samples were equilibrated for 1 min prior to each measurement. Only for the data presented in Figures 1 and 4 were the temperature increments 5 °C with at least 5 min equilibration each. Spectral simulations were performed using the DMfit software.[73]

Electron Microscopy: For electron microscopy the samples were frozen (from 12 °C) by plunging into liquid propane and freeze-fractured in a Balzers freeze-etching unit BAF 400 (BAL-TEC, Liechtenstein). The specimen surface was replicated by deposition of a platinum/carbon layer at an angle of incidence of 35° and a carbon support layer at 90°. Electron micrographs were taken at magnifications of 33 000 and 50 000 on a JEOL 100CX transmission electron microscope (Tokyo, Japan).

Acknowledgements

We thank Olaf Zwernemann, Stefanie Maurer and Silvia Gehrlein for peptide synthesis and purification, and the DFG and the Land Baden-Württemberg for financial support via the CFN (E1.2).

Keywords: lipids · membranes · micelles · NMR spectroscopy · peptides

[1] A. Pfeifer, I. M. Verma, *Annu. Rev. Genomics Hum. Genet.* **2001**, *2*, 177–211.
[2] H. Grosshans, *Funct. Integr. Genomics* **2000**, *1*, 142–145.
[3] W. F. Anderson, *Nature* **1998**, *392*, 25–30.
[4] H. M. Blau, M. L. Springer, *N. Engl. J. Med.* **1995**, *333*, 1204–1207.
[5] R. M. Mainardes, L. P. Silva, *Curr. Drug Targets* **2004**, *5*, 449–455.
[6] R. Langer, *Science* **1990**, *249*, 1527–1533.
[7] K. Lundstrom, T. Boulikas, *Technol. Cancer Res. Treat.* **2003**, *2*, 471–486.
[8] W. Walther, U. Stein, *Drugs* **2000**, *60*, 249–271.
[9] T. Niidome, L. Huang, *Gene Ther.* **2002**, *9*, 1647–1652.
[10] S. Mehier-Humbert, R. H. Guy, *Adv. Drug Delivery Rev.* **2005**, *57*, 733–753.
[11] D. J. Wells, *Gene Ther.* **2004**, *11*, 1363–1369.
[12] A. G. Schatzlein, *Anticancer Drugs* **2001**, *12*, 275–304.
[13] Y. Shoji, H. Nakashima, *Curr. Pharm. Des.* **2004**, *10*, 785–796.
[14] Y. M. Cho, J. D. Kim, K. Park, *Fundam. Clin. Pharmacol.* **2003**, *55*, 721–734.
[15] A. El-Aneed, *J. Controlled Release* **2004**, *94*, 1–14.
[16] S. El-Andaloussi, T. Holm, U. Langel, *Curr. Pharm. Des.* **2005**, *11*, 3597–3611.
[17] A. Joliot, A. Prochiantz, *Nat. Cell Biol.* **2004**, *6*, 189–196.
[18] S. Deshayes, M. C. Morris, G. Divita, F. Heitz, *Curr. Pharm. Des.* **2005**, *11*, 3629–3638.
[19] G. P. Dietz, M. Bahr, *Mol. Cell. Neurosci.* **2004**, *27*, 85–131.
[20] B. Gupta, T. S. Levchenko, V. P. Torchilin, *Adv. Drug Delivery Rev.* **2005**, *57*, 637–651.
[21] H. Brooks, B. Lebleu, E. Vives, *Adv. Drug Delivery Rev.* **2005**, *57*, 559–577.
[22] D. Derossi, S. Calvet, A. Trembleau, A. Brunissen, G. Chassaing, A. Prochiantz, *J. Biol. Chem.* **1996**, *271*, 18188–18193.
[23] R. Fischer, K. Kohler, M. Fotin-Mleczek, R. Brock, *J. Biol. Chem.* **2004**, *279*, 12625–12635.
[24] E. Vives, P. Brodin, B. Lebleu, *J. Biol. Chem.* **1997**, *272*, 16010–16017.
[25] S. Futaki, T. Suzuki, W. Ohashi, T. Yagami, S. Tanaka, K. Ueda, Y. Sugiura, *J. Biol. Chem.* **2001**, *276*, 5836–5840.
[26] E. Vives, *J. Mol. Recognit.* **2003**, *16*, 265–271.
[27] S. Futaki, *Adv. Drug Delivery Rev.* **2005**, *57*, 547–558.
[28] P. E. Thoren, D. Persson, P. Isakson, M. Goksor, A. Onfelt, B. Norden, *Biochem. Biophys. Res. Commun.* **2003**, *307*, 100–107.
[29] J. Oehlke, A. Scheller, B. Wiesner, E. Krause, M. Beyermann, E. Klauschenz, M. Melzig, M. Bienert, *Biochim. Biophys. Acta* **1998**, *1414*, 127–139.
[30] P. E. Thoren, D. Persson, E. K. Esbjorner, M. Goksor, P. Lincoln, B. Norden, *Biochemistry* **2004**, *43*, 3471–3489.
[31] J. P. Richard, K. Melikov, E. Vives, C. Ramos, B. Verbeure, M. J. Gait, L. V. Chernomordik, B. Lebleu, *J. Biol. Chem.* **2003**, *278*, 585–590.
[32] P. E. Thoren, D. Persson, P. Lincoln, B. Norden, *Biophys. Chem.* **2005**, *114*, 169–179.
[33] P. Curnow, H. Mellor, D. J. Stephens, M. Lorch, P. J. Booth, *Biochem. Soc. Symp.* **2005**, *72*, 199–209.
[34] J. S. Wadia, R. V. Stan, S. F. Dowdy, *Nat. Med.* **2004**, *10*, 310–315.
[35] I. M. Kaplan, J. S. Wadia, S. F. Dowdy, *J. Controlled Release* **2005**, *102*, 247–253.
[36] K. Melikov, L. V. Chernomordik, *Cell. Mol. Life Sci.* **2005**, *62*, 2739–2749.
[37] M. E. Herbig, U. Fromm, J. Leuenberger, U. Krauss, A. G. Beck-Sickinger, H. P. Merkle, *Biochim. Biophys. Acta* **2005**, *1712*, 197–211.
[38] M. Magzoub, L. E. Eriksson, A. Graslund, *Biophys. Chem.* **2003**, *103*, 271–288.
[39] B. Christiaens, S. Symoens, S. Verheyden, Y. Engelborghs, A. Joliot, A. Prochiantz, J. Vandekerckhove, M. Rosseneu, B. Vanloo, *Eur. J. Biochem.* **2002**, *269*, 2918–2926.
[40] M. Zasloff, *Nature* **2002**, *415*, 389–395.
[41] H. Binder, G. Lindblom, *Biophys. J.* **2003**, *85*, 982–995.
[42] N. Sakai, S. Matile, *J. Am. Chem. Soc.* **2003**, *125*, 14348–14356.
[43] J. C. Mai, H. Shen, S. C. Watkins, T. Cheng, P. D. Robbins, *J. Biol. Chem.* **2002**, *277*, 30208–30218.
[44] E. L. Snyder, S. F. Dowdy, *Pharm. Res.* **2004**, *21*, 389–393.
[45] N. Sakai, T. Takeuchi, S. Futaki, S. Matile, *ChemBioChem* **2004**, *5*, 114–122.
[46] M. Nishihara, F. Perret, T. Takeuchi, S. Futaki, A. N. Lazar, A. W. Coleman, N. Sakai, S. Matile, *Org. Biomol. Chem.* **2005**, *3*, 1659–1669.
[47] J. Mitchell, L. Steinman, D. T. Kim, C. G. Fatman, J. B. Rothbard, *J. Pept. Res.* **2000**, *52*, 318–325.
[48] C. P. Tilcock, P. R. Cullis, *Ann. N. Y. Acad. Sci.* **1987**, *492*, 88–102.
[49] S. M. Gruner, P. R. Cullis, M. J. Hope, C. P. Tilcock, *Annu. Rev. Biophys. Biophys. Chem.* **1985**, *14*, 211–238.
[50] V. L. Borovyagin, A. G. Sabelnikov, *Electron Microsc. Rev.* **1989**, *2*, 75–115.
[51] D. P. Siegel, *Biophys. J.* **1984**, *45*, 399–420.
[52] A. Ziegler, X. L. Blatter, A. Seelig, J. Seelig, *Biochemistry* **2003**, *42*, 9185–9194.

[53] R. N. Lewis, Y. P. Zhang, R. N. McElhaney, *Biochim. Biophys. Acta* **2005**, *1668*, 203 – 214.
[54] R. Koynova, M. Caffrey, *Biochim. Biophys. Acta* **1998**, *1376*, 91 – 145.
[55] S. Afonin, R. W. Glaser, M. Berditchevskaia, P. Wadhwani, K. H. Gührs, U. Möllmann, A. S. Ulrich, *ChemBioChem* **2003**, *4*, 1151 – 1163.
[56] A. S. Ulrich, P. Wadhwani, U. H. N. Dürr, S. Afonin, R. W. Glaser, E. Strandberg, P. Tremouilhac, C. Sachse, M. Berditchevskaia, S. L. Grage in *NMR Spectroscopy of Biological Solids* (Ed.: A. Ramamoorthy), CRC Press, Boca Raton, FL, **2006**, pp. 215 – 236.
[57] R. W. Glaser, C. Sachse, U. H. N. Dürr, P. Wadhwani, A. S. Ulrich, *J. Magn. Reson.* **2004**, *168*, 153 – 163.
[58] R. W. Glaser, C. Sachse, U. H. N. Dürr, P. Wadhwani, S. Afonin, E. Strandberg, A. S. Ulrich, *Biophys. J.* **2005**, *88*, 3392 – 3397.
[59] E. Strandberg, P. Wadhwani, P. Tremouilhac, U. H. N. Dürr, A. S. Ulrich, *Biophys. J.* **2006**, *90*, 1676 – 1686.
[60] P. Wadhwani, S. Afonin, M. Ieronimo, J. Bürck, A. S. Ulrich, *J. Org. Chem.* **2006**, *71*, 55 – 61.
[61] A. S. Ulrich, *Prog. Nucl. Magn. Reson. Spectrosc.* **2005**, *46*, 1 – 21.
[62] J. Salgado, S. L. Grage, L. H. Kondejewski, R. S. Hodges, R. N. McElhanye, A. S. Ulrich, *J. Biomol. NMR* **2001**, *21*, 191 – 208.
[63] A. S. Ulrich, M. Otter, C. G. Glabe, D. Hoekstra, *J. Biol. Chem.* **1998**, *273*, 16748 – 16755.
[64] R. W. Glaser, M. Grüne, C. Wandelt, A. S. Ulrich, *Biochemistry* **1999**, *38*, 2560 – 2569.
[65] S. Afonin, U. H. N. Dürr, R. W. Glaser, A. S. Ulrich, *Magn. Reson. Chem.* **2004**, *42*, 195 – 203.
[66] S. Jiang, Q. Zhao, A. K. Debnath, *Curr. Pharm. Des.* **2002**, *8*, 563 – 580.
[67] F. Picard, M. J. Paquet, J. Levesque, A. Belanger, M. Auger, *Biophys. J.* **1999**, *77*, 888 – 902.
[68] K. Han, M. J. Jeon, S. H. Kim, D. Ki, J. H. Bahn, K. S. Lee, J. Park, S. Y. Choi, *Mol. Cells* **2001**, *12*, 267 – 271.
[69] Y. N. Kaznessis, S. Kim, R. G. Larson, *J. Mol. Biol.* **2002**, *322*, 569 – 582.
[70] B. B. Bonev, Y.-H. Lam, G. Anderluh, A. Watts, R. S. Norton, F. Separovich, *Biophys. J.* **2003**, *84*, 2382 – 2392.
[71] J. L. Nieva, R. Bron, J. Corver, J. Wilschut, *EMBO J.* **2004**, *13*, 2797 – 2804.
[72] S. Afonin, U. H. N. Dürr, P. Wadhwani, J. Salgado, A. S. Ulrich, unpublished results.
[73] D. Massiot, F. Fayon, M. Capron, I. King, S. Le Calvé, B. Alonso, J-O. Durand, B. Bujoli, Z. Gan, G. Hoatson, *Magn. Reson. Chem.* **2002**, *40*, 70 – 76.

Received: May 18, 2006
Published online on September 20, 2006

